

# Multi-objective Optimization and Sensitivity Analysis of the Parameters Affecting Sealing Performance of the Piston Rings Face through the Validated Model for the Four-stroke Bi-fuel Engine

A. Q. Almansoori<sup>1</sup>, A. Hajjalimohammadi<sup>2†</sup>, S. M. Agha Mirsalim<sup>1</sup> and M. Mehrabivaghar<sup>3</sup>

<sup>1</sup>Department Of Mechanical Engineering, Amirkabir University Of Technology, 424 Hafez Avenue, Po Box 15875-4413, Tehran, Iran

<sup>2</sup> Faculty of Mechanical Engineering, Semnan University, Semnan, 35131-19111, Iran

<sup>3</sup>Engine Labs Unit, Irankhodro Powertrain Company (IPCO), Tehran, 13988-13711 Iran

† Corresponding Author Email: [ahajjali@semnan.ac.ir](mailto:ahajjali@semnan.ac.ir)

(Received January 8, 2022; accepted May 18, 2022)

## ABSTRACT

A multi-objective optimization study and sensitivity analysis of a SI engine piston-rings pack using dynamics analysis software (AVLExcite Piston&Rings) and optimizer software (modeFRONTIER) are presented. The effects of changing the piston rings' tangential force and face profile on the oil and gas flow behavior inside the piston-rings pack are investigated by calculating the lubrication oil consumption, blow-by, and power losses. The feasibility of the simulation model was determined by comparing it to empirical data obtained from experimental testing of the engine to estimate the amount of oil consumption and blow-by gas flow. Using the statistical modeling algorithm SS-ANOVA, multi-objective optimization investigates the individual and interaction effects of the three rings' tangential forces. This method significantly reduces the time and cost required to find the optimal design, an approach not reported in previous studies. The results showed a strong correlation between simulation and experimental test results, indicating an acceptable match during model validation. Furthermore, the predictions show that tangential forces affect sealing performance; thus, modifying the tangential force resulted in a 30% reduction in oil consumption and less than a 0.8 percent increase in friction. Furthermore, the LKZ oil control ring model efficiently reduces oil consumption by 25% while slightly increasing friction (about 10 percent without face coating).

**Keywords:** Internal combustion engines; Blow-by, power loss; Friction; Lubrication oil consumption; Multi-objective optimization; AVLExcite; modeFRONTIER.

## NOMENCLATURE

|              |                                                 |            |                                           |
|--------------|-------------------------------------------------|------------|-------------------------------------------|
| a            | ring radial width                               | F          | force                                     |
| A            | film surface area                               | h          | oil film thickness                        |
| B            | cylinder bore                                   | I          | area moment of inertia                    |
| b            | ring thickness                                  | l          | ring perimeter                            |
| BBY          | blowby gas                                      | LOC        | Lubrication Oil Consumption               |
| $c_{\infty}$ | concentration of lube oil in combustion chamber | m          | mass flow rate                            |
| $c_{film}$   | concentration of lube oil at film surface       | MOO        | Multi-objective Optimization              |
| d            | ring diameter                                   | P          | pressure                                  |
| $D_c$        | diffusion coefficient                           | PL         | friction power loss                       |
| E            | modulus of elasticity                           | R          | gas constant                              |
| FMEP         | Fraction Mean Effective Pressure                | r          | ring radius                               |
|              |                                                 | $s_{film}$ | movement of the piston during a time step |
|              |                                                 | T          | temperature                               |

|                  |                                   |        |                            |
|------------------|-----------------------------------|--------|----------------------------|
| $V_p$            | piston reciprocating speed        |        | the oil film               |
| $\beta$          | material transmission coefficient | $\phi$ | crank angle                |
| $\Delta s$       | uncovered area of the oil film    | $\mu$  | viscosity of the lubricant |
| $\Delta \bar{u}$ | mean difference velocity of       | $\psi$ | gas flow coefficient       |

## 1. INTRODUCTION

In recent years, the entry of hybrid cars into the powertrain market, as well as difficulties resulting from international organizations' requirements imposed to reduce environmental pollution, are the main challenges that internal combustion engine manufacturers have faced in order to stay competitive. As a result, reducing emissions and increasing engine efficiency became a major focus for researchers.

The piston-rings pack's primary function is to prevent lubricant oil consumption and combustion chamber gas leakage (Ahmed Ali *et al.* 2016; Sohrabiasl *et al.* 2017). In other words, aside from the sealing process the piston reciprocating movement presents a challenge for investigators and engine manufacturers due to difficulties in controlling friction and wear (Rahmani *et al.* 2017; Gholami *et al.* 2020; Saligheh *et al.* 2020).

In general, most of the oil consumed is converted into unburned hydrocarbons and particle matter released with exhaust gases. The engine lubricant also serves as a source of precipitates inside the cylinder, resulting in failures such as pre-ignition and engine knocking (Di Battista and Cipollone 2016; Almansoori *et al.* 2017). According to studies, the piston and cylinder system is responsible for 70-80% of oil consumption sources in the engine (Froelund *et al.* 2004; Smith 2011). Thus, optimizing the structural parameters that influence the lubrication oil consumption rate and blow-by gasses is essential. This topic has attracted the attention of a large number of researchers, some of whom will be cited in this paper.

Evaluating lubrication oil film thickness changes with engine speed is fundamental to understanding different friction principles, oil distribution, and gas flow. Concurrently, viscosity and pressure are controlled (Kirner *et al.* 2016). Therefore, determining the ring face forces and lubricating oil layer thickness between the piston and cylinder liner is sensible. (Tian *et al.* 1996), used the average flow model to develop one of the most extensive oil transport models (Patir *et al.* 1979). By solving the Reynolds equation for a compressible piezo-viscous fluid, a 1D model can predict the lubricant oil layer thickness. Later, the model was expanded to include all rings, assuming that the oil control ring would typically be available during the piston's downstroke. Reynolds' equation controls the ring pack's incompressible fluid pressure generation. This was demonstrated by a small amount of oil being carried by the top ring during the compression stroke. The

surface roughness also contributes to lubricant transition (Dolatabadi *et al.* 2020).

A multi-physics integrated model to analyze the effects of transient ring electrostatics, gas flow through piston clearances caused by gas pressure leakage from the combustion chamber, and friction energy losses are introduced (Kaliappan *et al.* 2019; Turnbull *et al.* 2020). The results show that the impact of ring dynamics and blow-by on surface contact geometry, lubricant film distribution, and friction calculation cannot be ignored. It was also observed that the energy loss by blow-by is equal to six times higher than frictional power loss in engines generated by piston and ring dynamics.

The friction coefficient is proportional to the film thickness. (Abu-Nada *et al.* 2008) approximated the lubricating layer thickness and oil distribution on the cylinder wall, as the minimum thickness appears top and bottom dead center, while the maximum thickness appears in the middle of the stroke with a value ranging from 2.5 to 8 mm. (Zhang *et al.* 2016) presented an optimization study of the top piston ring face profile using the sequential Quadratic Programming (SQP) method, which was introduced and validated by (Elsharkawy and Alyaqout 2009). It was discovered that the shape of the ring face controls the distribution of the oil layer at the ring-bore interface. As a result, the steep profile of the top ring face reduces friction. (Mishra *et al.* 2019) introduced an optimization model for piston crown geometry using structural strength and lubrication performance correlation analysis. It was determined that the effects of all studied forces should be taken into account during the finite element simulation method. Additionally, combining the numerical contact model and the finite element method for structural strength suggests several critical conclusions.

(Miao *et al.* 2020) developed a piston-ring pack optimization technique for analyzing lubrication oil consumption. AVL Excite Piston & Ring was used to simulate different issues such as the thermodynamic boundary conditions, oil consumption, piston dynamic, and piston ring dynamic. The model outputs were compared with the available test results of a diesel engine to verify the validation of the study. The outcomes showed that results could be recognized as references for additional piston and piston ring design improvements.

The genetic algorithm is a sophisticated, extremely robust, multi-objective algorithm developed recently to simulate natural selection and reproduction as an optimization concept for determining the optimal

design (Gunantara 2018). Typically, optimizing systems in internal combustion engines results in an area of design optimization to achieve the best performance. Typically, classical optimization is used to solve a single-objective problem. Indeed, it will always involve extremely complex and non-linear models, particularly in engineering applications. In reality, engineering phenomena are invariably characterized by non-linear and complex models (Mohiuddin *et al.* 2011). As a result, multi-objective optimization is a well-established technique for resolving this engineering problem.

In mechanical problems, several studies used a multi-objective genetic algorithm and the Mode Frontier optimizer to provide a sensitivity and optimization study, especially concerning the integrative node of synchronizing the Optimizer with different CAE software (Jena 2013; Jahromi 2014; Clarich *et al.* 2016).

(Usman *et al.* 2015) investigated a two-dimensional elastohydrodynamic lubrication model under fully lubricated conditions. For an internal combustion engine cycle, several liner profiles were evaluated for conformability, oil layer thickness, friction power loss, and lubrication oil flow. The liner distortion sensitivity analysis was introduced in this paper to understand better two-dimensional PRL lubrication and its implications for design optimization and decision making.

The GT-Suite software was used to study one-dimensional hydrodynamic lubrication between the compression ring and the liner (Menacer *et al.* 2020). The method was used to evaluate the sensitivity of different ring' designs to system performance. They discovered that modifying the top ring profile reduced frictional power losses while improving tribological properties.

Although numerous studies have established that optimizing the design of piston rings assemblies through theoretical and practical experiments, particularly optimization methods, has a significant effect on increasing their efficiency, few papers (almost none) report the sensitivity of design factors to system performance has an interactional effect. Additionally, conducting experimental tests with multiple ring designs is costly. As a result, the contribution of this paper falls into two aspects. First, the paper used a genetic algorithm to study the sensitivity of a group of factors. Second, design a simulation-based multiple objectives optimization approach to improve the design of a piston ring pack. Studying the tangential force interaction effect across all rings is more effective than studying each ring separately. This method reduces the time required to study each objective separately. It also saves the high cost of testing different models on the engine to find the best design. The study also examined the effectiveness of a new lubrication ring design (LKZ oil control ring).

The current article focuses on multi-objective optimization and sensitivity analysis of the piston-ring pack in order to provide an integrated conceptualization of the friction-sealing efficiency trade-offs via factors analysis. As a novel concept,

the AVLExcite and ModeFRONTIER software were combined to investigate the individual and combined effects of ring face force and geometry on lubrication oil consumption, blow-by, and friction power loss. Then, based on the results, the optimal design of the piston ring pack was proposed.

## 2. METHODOLOGY

### 2.1. Ring-pack Modeling Approach

The piston ring dynamics model was used to simulate a four-stroke gasoline engine operating at full load. The model was employed to analyze the effects of rings radial force and geometry design on lubrication oil consumption, the blow-by, and friction power loss. The piston and ring assembly system consist of two compression rings, the oil control ring, the piston, and the cylinder liner, as shown in Fig. 1.

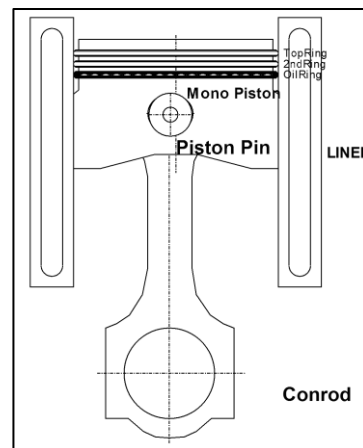


Fig. 1. schematic diagram of the piston rings assembly.

The piston and cylinder assembly simulation depends on analyzing the forces acting on the ring in both axial and radial directions during the engine cycle. These forces generate resistance to prevent oil and gas leakage to the combustion chamber and the crankcase. On the other hand, these forces cause power loss due to friction between the contact surfaces. Forces and moments applying to a ring through the combustion cycle are illustrated in Fig. 2. The forces exerted on the surface of the piston play a major role in calculating the amount of oil consumption, gas leakage, and the amount of friction between surfaces during movement.

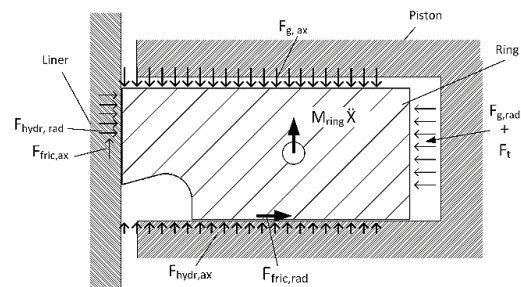


Fig. 2. Forces acting on piston rings.

The piston ring dynamics module considers forces and moments, friction, and the blow-by gas flow from the combustion chamber through the rings' clearance to the crankcase to calculate the net force acting upon the rings. The piston ring is subject to three inertia, pressure, and contact forces (GmbH, 2016a).

The axial forces applied to the ring act as a contact force  $F_{\text{contact}}$  and are equal to:

$$F_{\text{contact,ax}} = (F_{\text{gas}} + F_{\text{mass}} + F_{\text{fric}} + F_{\text{bend}})_{\text{ax}} \quad (1)$$

The symbols  $F_g, F_{\text{mass}}, F_{\text{fric}}$  and  $F_{\text{bend}}$  are gas force, mass force, friction force, and bending force, respectively.

Through identifying the equilibrium of axial forces applied to the ring faces, the equation of motion is formulated as follows:

$$m_{\text{ring}} \ddot{x} = \sum F = (F_g + F_{\text{hydr}} + F_{\text{fric}} + F_{\text{bend}})_{\text{ax}} \quad (2)$$

Where  $m_{\text{ring}} \ddot{x}$  is mass force (including gravity and piston tilting motion). The radial contact forces (hydrodynamic forces  $F_{\text{hydr}}$ ) between the liner and rings face are given by:

$$F_{\text{hydr,rad}} = (F_g + F_t + F_{\text{fric}})_{\text{rad}} \quad (3)$$

Where  $F_t$  is ring tangential force.

The gas force acts behind the inner side of the ring obtained from the combustion chamber pressure through the following equation.

$$F_{\text{gas}} = P_{\text{gas}} b l \quad (4)$$

Where  $p_{\text{gas}}$  is gas in-cylinder pressure,  $b$  is Ring thickness, and  $l$  is Ring perimeter.

Moreover, the elastic ring tension force (tangential force) is determined as a function of the elastic pressure (Lu *et al.*, 2018; Bewsher *et al.*, 2019);

$$F_t = P_c b d \quad (5)$$

$$P_c = \frac{gEI}{3\pi b r^3} \quad (6)$$

$$I = \frac{b d^3}{12} \quad (7)$$

Substituting Eqs. (6) and (7) in (5)

$$F_t = \frac{gEba^3}{36\pi r^3} \quad (8)$$

$P_c$  is contact pressure

$d$  is ring diameter and radius

$r$  is ring radius

$a$  is ring radial width

For the analysis of lubrication in a piston ring pack, in order to calculate the hydrodynamic force effect and the pressure distribution behind the ring, the

two-dimensional Reynolds equation for a compressible piezo-viscous fluid can be simplified to an ordinary differential equation.

$$\frac{\partial}{\partial x} \left( h^3 \frac{\partial P}{\partial x} \right) = 6\mu V_p \frac{\partial h}{\partial x} + 12\mu \frac{\partial h}{\partial t} \quad (9)$$

Parameter  $h$  is oil film thickness,  $\mu$  is the viscosity of the lubricant,  $V_p$  is piston reciprocating speed, and can be obtained from the following equation:

$$V_p = -r\omega \sin \varphi \left\{ 1 + \cos \varphi \left[ \left( \frac{l}{r} \right)^2 - \sin^2 \varphi \right]^{-0.5} \right\} \quad (10)$$

Where  $\varphi$  is crank angle and  $\omega$  is crank RPM. The solution procedure applied for solving the Reynolds equation keeps the boundary conditions according to Reynolds and utilizes the cavitation zone pressure gradient of the gap area (GmbH, 2016a):

$$\begin{cases} P_{x=x_{cr}} = P_{cav} \\ \left. \frac{dp}{dx} \right|_{x=x_{cr}} = 0 \end{cases} \quad (11)$$

$P_{cav}$  is cavitation pressure. The height of the lubrication gap will be acquired iteratively, the load-carrying capacity of the lubricating film having to balance the total of the forces acting upon the ring in the radial direction.

## 2.2. Lube Oil Consumption Calculation

The lubrication oil consumption model estimates two mechanisms; the first mechanism is the evaporation of the oil film from the liner surface, and the second mechanism is the oil throw-off or the oil consumed inside the combustion chamber, which happens due to different reasons like (GmbH, 2016a);

- Oil throw-off of accumulated oil above the top ring due to ring scraping and the effect of inertia force.
- Oil blow-back over the surfaces and through the end gap of the top ring into the combustion chamber at the intake stroke due to a negative pressure gradient.

According to the data from the pre-calculation of piston and ring dynamics, the lube oil consumption module considers different oil film thicknesses.

The evaporation of lubrication oil from the liner is estimated by calculating the amount of the lubricant oil that evaporates from the liner wall (diffusion process) during the combustion process Fig. 3 (Soejima *et al.*, 2017; Qian *et al.*, 2020). Steady-state convective mass transfer is applied to achieve the evaporation rate:

$$\dot{m}_{\text{evap.oil}} = A \frac{\beta P_{\text{film}}(t, s)}{RT_{\text{film}}(t, s)} \quad (12)$$

Where  $A = \pi B \Delta s$  (The film surface area),  $\Delta s$  is the movement of the piston during the time step,  $B$  is cylinder bore,  $\beta$  is material transmission coefficient,  $P_{\text{film}}$  is oil film pressure, and  $T_{\text{film}}$  is oil film temperature.

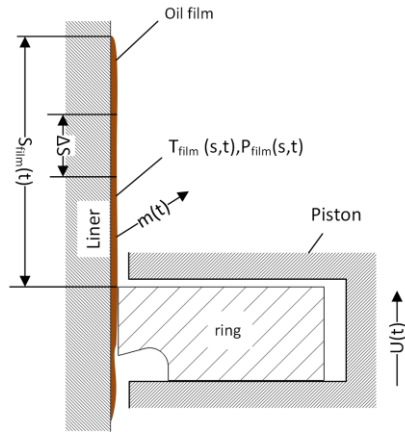


**Fig. 3. Oil Mass Flow to Combustion Chamber.**

The total evaporated mass in one cycle can be found by integrating the mass given in Eq. 12 over one combustion cycle, as follows;

$$M_{oil} = \int_{cycle} \dot{M}_{evap,oil}(t) dt = \frac{\pi B^2 \sum_0^{\theta} \beta(s,t) P_{film}(s,t)}{R T_{film}(s,t)} \Delta s \quad (13)$$

On the other hand, the thrown-off oil quantity is determined by the oil volume above the top ring through the flow balance of lube oil between the top land and liner and the consideration of the piston acceleration. The following transport mechanisms lead to a rate of change of the oil mass above the top piston ring Fig. 4.

$$\dot{m}_{acc}(t) = (\dot{m}_{scr} + \dot{m}_{pmp,top} - \dot{m}_{blw}) \Delta t \quad (14)$$

where

$\dot{m}_{acc}$  is mass flow rate of accumulated oil between top land and liner wall

$\dot{m}_{scr}$  mass flow rate of oil scraped by the top ring

$\dot{m}_{pmp}$  mass flow rate of oil pumped at the passage of the top flank of top ring

$\dot{m}_{blw}$  oil mass flow rate blow down the top ring

For estimating the amount of oil throw-off ( $\dot{V}_{throw-off}$ ) from the accumulated oil between the piston top land and the liner wall, the following model can be used (GmbH, 2016a);

$$\dot{V}_{throw-off} = \Delta \bar{u} h d_{film} \pi \Delta t \quad (15)$$

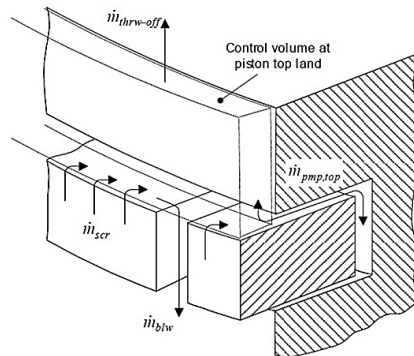


**Fig. 4. Oil flow at piston top land (GmbH, 2016a).**

### 2.3. Gas Flow Model (blow-by)

Through the power stroke, the high pressure inside the combustion chamber leads to combustion gases leakage into the crevices between the piston ring, piston grooves, and the liner. For calculating the gas forces acting upon the piston rings, the pressures resulting from the gas flow have to be known. Therefore, the entire ring pack volumes have been divided into chambers (gaps in the grooves and lands between the rings) connected by a throttling point. The gas flow through the chambers is assumed to be the isentropic orifice flow and can be solved as (GmbH 2016a; Turnbull *et al.* 2020):

$$\dot{m} = A \psi p_c \sqrt{\frac{2}{RT_c}} \sqrt{\frac{\kappa}{\kappa-1} \left[ \left( \frac{p_0}{p_c} \right)^{2/\kappa} - \left( \frac{p_0}{p_c} \right)^{\kappa+1/\kappa} \right]} \quad (16)$$

$$\Delta m = \dot{m} \Delta t \quad (17)$$

$$p_c = \frac{RT_c}{V_c} (m + \Delta m) \quad (18)$$

Where  $p_c$  is the pressure of the divided chambers,  $p_0$  is the pressure of the chambers surrounding,  $\psi$  is the gas flow coefficient, and  $\kappa$  is a polytropic exponent. and  $R$  is the constant of the evaporated oil (gas constant).

### 2.4. Multi-Objective Genetic Algorithm (MOGA) Solution with ModeFRONTIER

The primary objective of conducting an optimization study with the ModeFRONTIER program is to automate design evaluations and optimize the process. The process summarized in Fig. 5 consists of defining the input parameters, running the simulation, reading the results, and defining the design to be evaluated next. Then the loop is repeated until an optimum level is found or, more commonly, good enough results are obtained.

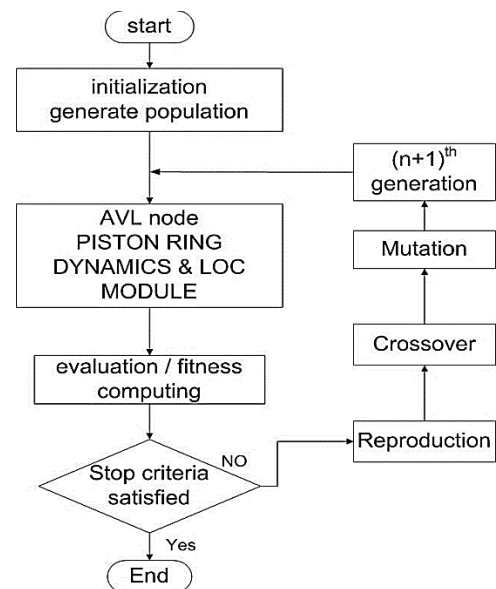


**Fig. 5. General algorithm flow chart of modeFRONTIER.**

Genetic Algorithm (GA) is part of the new field research term in evolutionary computation, which has influential exploration and optimization abilities (Venkataraman 2009).

The specific version of the multi-objective genetic algorithm used in this study is MOGA-II which applies intelligent and effective multi-search elitism to maintain excellent solutions converging precipitately to an optimum solution. Elitism enhances the convergence of the algorithm and confirms that the fitness of the new generation is more inclusive than the fitness of the parent generation.

ModeFRONTIER has three environments: Workflow Editor, Run Analysis, and Design Space. The first step is to create a graphical problem description (workflow environment in Fig. 6). It shows the simulations, the applications, and their order. The "how" indicates your choice of measures (inputs and outputs), optimization objectives, and design space exploration and optimization algorithms.

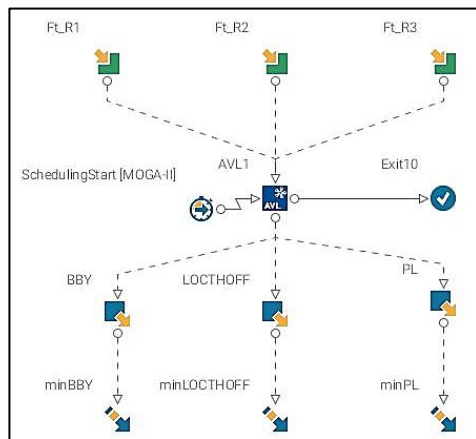


**Fig. 6. Modefrontier Workflow.**

In order to find the sensitivity of various factors to the objectives, the statistical analysis has the ability to identify global correlations and main and interaction effects of dependent and independent variables. As a result of the statistical analysis, the problem dimension can be reduced by excluding unimportant factors.

The AVL-AST node is a CAE node integrating AVL software with modeFRONTIER, transferring data between the two software. The node helps to find synchronization between the AVLExcite and modeFRONTIER, where the piston-ring system is simulated, and the values of oil consumption, blow-by, and friction power loss are calculated.

The study is divided into two parts; the first is to study the behavior of oil consumption, friction, and Blowby gasses by changing the rings tangential force values individually and changing the face profile of the third ring. The next section is studying the sensitivity and selecting the optimum design, using the multi-objective genetic algorithm through

synchronizing the AVLExcite and modeFRONTIER software.

### 3. RESULTS AND DISCUSSION

#### 3.1. Simulation Parameters

The sensitivity of the factors affecting the sealing process must be studied to improve ring pack sealing efficiency. The lubricating oil and gas flow through the gaps between the ring, piston, and liner surfaces. Reducing oil and gas leakage requires understanding the sensitivity of the influencing factors and optimizing design. The ring tangential force affects both sealing and friction. This force is affected by the ring's design, type, and surface coating. The sensitivity of some factors such as the ring tangential force and the lubricating control ring face profile has been calculated using the above model to improve the sealing effect and friction. The flowchart of the model is explained in Fig. 5. A typical 4-stroke 4-cylinder gasoline engine at 4000 rpm has been considered in this study. The simulation was run under the engine conditions described in Table 1, where the data provided by the original engine manufacturer (IPCO).

**Table 1 Engine technical specification**

| Parameters                  | Values   |      |               |
|-----------------------------|----------|------|---------------|
| <b>Engine details</b>       |          |      |               |
| Bore                        | 78.6 mm  |      |               |
| Stroke                      | 85 mm    |      |               |
| Nominal Displacement        | 1700 cm3 |      |               |
| <b>Operating conditions</b> |          |      |               |
| Load (Nm)                   | 113      |      |               |
| Speed (rpm)                 | 4000     |      |               |
| Oil type                    | 10W40    |      |               |
| <b>Rings specification</b>  | Top      | 2nd  | Oil           |
| Ring radial width (mm)      | 2.9      | 3.25 | 2.35          |
| Ring thickness (mm)         | 1.2      | 1.5  | 2.5           |
| <b>Ring-type</b>            | B        | NM   | Spring loaded |

The value of the tangential force of the first and second rings is calculated according to Eq. (8). Moreover, it can be estimated according to ring standards, taking into account the corrective factors related to the elasticity of the material, the design of the ring cross-section, and the surface treatment.

Depending on the tangential force equation, three design factors affect the magnitude of this parameter: the ring end gap, radial thickness, and ring width. Fig. 7. shows the effect of each of the factors mentioned above on the tangential force. The close gap effect is insignificant, as shown in Fig. 7 a, while the width and thickness of the ring directly affect the quantity of the force. According to ring standard, changing ring thickness from 2.9 to 3.6 mm and the width from 1.2 to 2.5 mm increases the forces by 7 and 8.5 N, respectively (Fig. 7 b, c). Thus, to change the value of the tangential force, some ring design

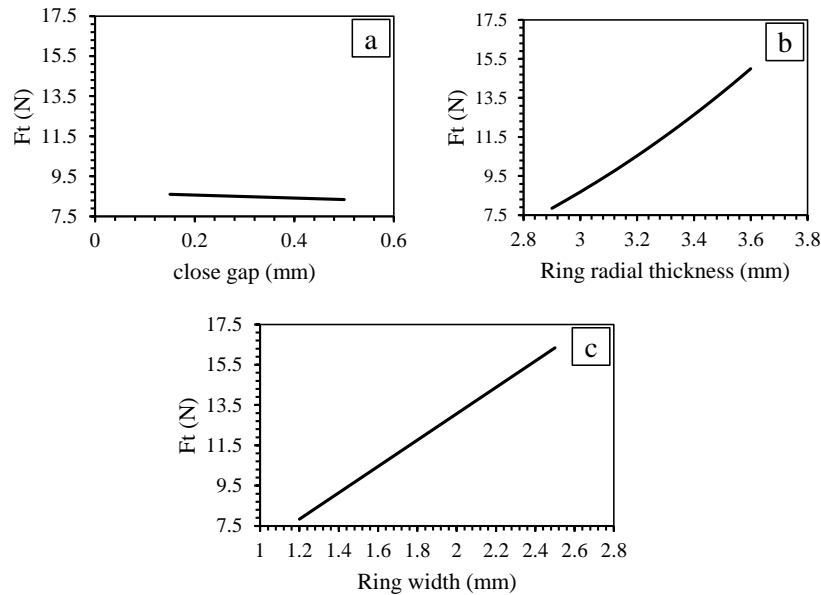


**Fig. 7. EFFECT of (a) end gap, (b) radial ring thickness, and (c) ring width on tangential force value.**

factors must be adjusted, which may impact the lubrication oil consumption and friction.

On the other hand, increasing the tangential force involves considering the dimensions change impact on friction and oil consumption. The parametric effect of changing the ring's dimensions on the system's performance was studied. Increasing the first ring's height from 1.2 to 2.5 increases friction and oil consumption by around 6%. While increasing the thickness of the same ring has a negligible effect on friction and does not affect the amount of oil consumed. Thus, to avoid friction loss, the thickness of the ring must be changed at a rate greater than its height.

The percentage change in the value of the tangential forces permitted is  $\pm 20\%$  depending on the type and dimensions of the rings studied. Whereas the standard permissible ring dimensions and the use of Eq. (8) to calculate tangential force resulted in the determination of the range of the first and second rings force applied in this study, which is listed in Table 2. It should be noted that the default values shown in the table are the average real value of the tangential forces of the simulated engine, which have been applied in the model validation. Furthermore, the specified range value is the range of the tangential force defined to perform the sensitivity analysis and the optimization study.

**Table 2 Tangential forces defined range**

| The Ring Ft              | Default value | Defined range |
|--------------------------|---------------|---------------|
| Top ring (N)             | 8.5           | 5-15          |
| 2 <sup>nd</sup> ring (N) | 8             | 5-13          |
| Oil ring (N)             | 25            | 15-49         |

As for the spring-loaded oil control ring, the calculation of the tangential force differs due to the presence of the spring that generates additional forces. Essentially, it is calculated depending on the

amount of contact pressure  $P_c$ . The contact pressure value can be chosen in a wide range according to the requirements and application of the rings. According to ISO 6626-2:2013 standard, the contact pressure range is subdivided into six classes, as listed in Table 3. Concerning the purpose of this investigation and the above details, the third ring tangential force required range was determined and listed in Table 2. Considering that the PNV Type of force has been neglected, it is unusable for the studied oil ring model.

**Table 3 classes of nominal contact pressure**

| Class | Meaning                           |
|-------|-----------------------------------|
| PNE   | Very low nominal contact pressure |
| PNL   | Low nominal contact pressure      |
| PNR   | Reduced nominal contact pressure  |
| PNM   | Medium nominal contact pressure   |
| PNH   | High nominal contact pressure     |
| PNV   | Very nominal contact pressure     |

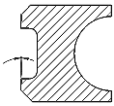
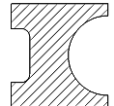
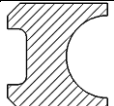
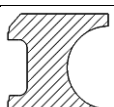
The AVL node's parameter-chooser detects the input and output parameters set in the AVL software optimization setting. It can either establish links between those parameters and existing modeFRONTIER variable nodes. As listed in Table 4, This study defines three input parameters and three output responses connected as objective nodes in the workflow environment.

**Table 4 Input and output variables**

| Node name          | Description                   |
|--------------------|-------------------------------|
| Input nodes        |                               |
| Ft_R1              | The 1st ring tangential force |
| Ft_R2              | The 2nd ring tangential force |
| Ft_R3              | The 3rd ring tangential force |
| Response variables |                               |
| LOCTHOFF           | Throw off oil consumption     |
| BBY                | Blow-by gasses                |
| PL                 | Friction power loss           |

On the other hand, the ring face profile design's sensitivity has been studied by comparing the default design of the third ring with three different models according to the IOS6624 standard, as listed in Table 5. One of them is the LKZ design. LKZ oil control ring is considered one of the most efficient designs proposed in 2011 by Federal-Mogul to reduce lubricant oil consumption by keeping the friction power loss at an acceptable level utilizing face coating (Powertrain 2010). Thus, this design was used to study its effect without coating.

**Table 5 Studied oil control ring models**

| Model | Description                                      | Section                                                                            |
|-------|--------------------------------------------------|------------------------------------------------------------------------------------|
| DEF   | Default model of this study                      |   |
| SSF   | Coil spring loaded Slotted oil control ring      |   |
| DSF   | Coil spring loaded beveled-edge oil control ring |   |
| LKZ   | LKZ Taper Land Oil Control Ring                  |  |

**3.2. Validation of Simulation Results**

The EF7 gasoline engine was considered in the present study. The technical specifications of the engine investigated in this paper are shown in Table 1. The experimental tests were carried out in the Iran Khodro Engine Research Center (IPCO).

The direct weighing method measured the oil consumption rate based on the Renault test procedure. The measurement was conducted by monitoring the oil mass balance inside the sump after the engine was running for a specific time. As a result of the weighted method's inability to include leaked oil from other engine parts, as well as the long measurement times required to perform the test, it is less accurate than the absolute LOC value.

The LOC was calculated by the mean value of different tests that have been done on the same type of engine and the same running condition. The test was carried out for the engine with a part load and speed of 4000rpm. The test duration was four-hours with the following procedure:

- Start the engine for +30 sec idling.
- Increase the engine speed corresponding to engine torque (Nm) to the test condition (part-load and 4000 rpm) for 4 hours
- 15-sec idling
- Stop the engine in its natural position
- Oil flow during 20 min ± 1 min (draining)
- Calculate the weight of the drained oil through a smart digital scale

Furthermore, The AVL 442 Blow-by meter has been used to measure the leaking gas volume flow rate. The blow-by measurement device consists of an orifice measuring pipe and evaluation electronics to offer high accuracy determinations in both directions. The steadying vessels confirm measurement reliability even when measuring intensive pulsating blow-by flows. The gas flow rate calculation is achieved by determining the gas pressure gradient in front of and after the orifice using a differential pressure transducer, as shown in Fig. 8.

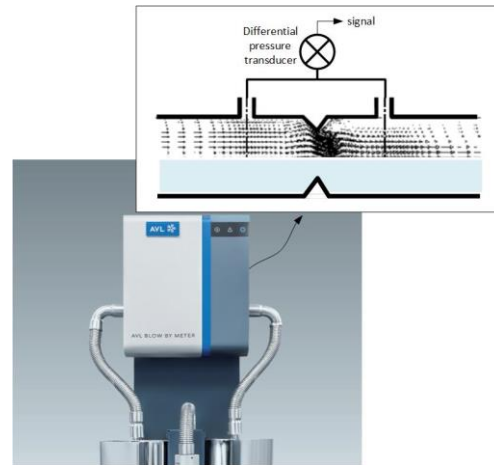


**Fig. 8. AVL blow by meter.**

**Table 6 Engine operation condition results (blow-by test)**

| Parameters                   | Values |
|------------------------------|--------|
| Speed (rpm)                  | 4000   |
| Fuel Consumption (kg/hr)     | 16.1   |
| Ambient Air Temperature (°C) | 30     |
| Ambient Air Pressure (kPa)   | 88.6   |
| Intake Air Temperature (°C)  | 27     |
| Intake Air Pressure (kPa)    | 100    |
| Blow-by pressure (kPa)       | -1.8   |
| Blow-by temperature (°C)     | 33     |
| Crankcase Pressure (kPa)     | 0.2    |
| Oil temperature (°C)         | 90     |
| Coolant temperature (°C)     | 90     |

In order to measure the blow-by gas flow rate, an AVL442 blow-by meter was directly connected to the engine blow-by circuit. The test operation conditions were performed at 4000 rpm speed and part load with 113 Nm torque. As illustrated in Schematic Fig. 9, the setup circuit is composed of numerous components, including the oil separator and the PCV valve. Along with measuring the gas flow rate, the engine measurement system incorporates additional sensors to monitor the engine's various operating conditions, such as pressures, temperatures, and fuel consumption rate, as detailed in Table 6, where the complete experimental setup for the EF7 engine is depicted in Fig. 10.



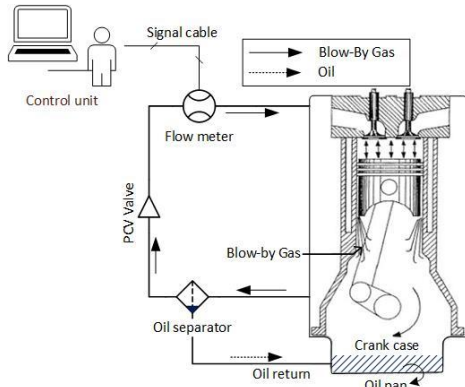


**Fig. 9. Schematic diagram of blow-by measurement circuit.**

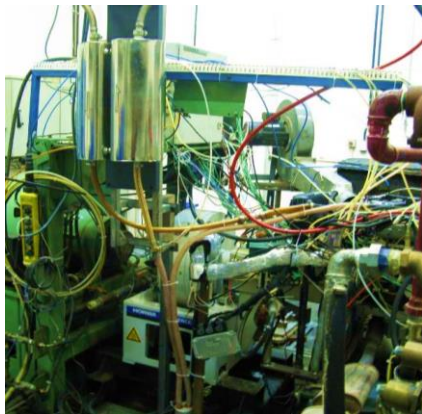


**Fig. 10. AVL442 blow-by meter and sensors connected to the engine.**

The AVL Excite simulation method has been used to provide piston-rings design guidelines. Therefore, simulated lubrication oil consumption and blow-by were calibrated based on the value of the experimental results. Fig. 11 compares experimental and simulated oil consumption and blow-by results. The present simulation results are acceptable and credible because the simulation model accurately captures lube oil consumption and blow-by in tests. It should be remarked that the LOC simulation results have about 4% error compared with experimental data. This variation in oil consumption in the engine represents the reality that cannot be simulated. These factors include oil consumption in other parts of the engine, such as the cylinder head, and oil leakage from various parts of the engine. Nonetheless, the present simulation results are valid and reliable for system performance improvement.

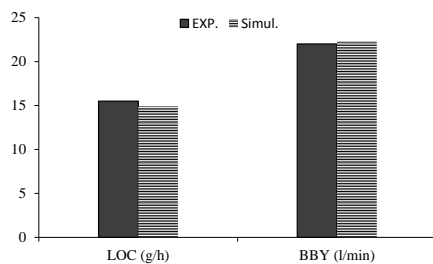


**Fig. 11. Comparison of predicted and measured LOC and BBY.**

Furthermore, the oil consumption results for different speeds and loads were not obtained because of laboratory and standard constraints. As a result, the theoretical and practical findings of friction behavior were compared in order to validate the simulations for different engine speeds. Frictional testing was carried out in the current study using a driving test cell. The friction value for each test was determined using the engine friction mean effective pressure (FMEP). Because of friction in engine components, the engine must be spun with a certain amount of torque. This torque, which is provided by an electric motor, is measured using a torque flange device (Vaghar *et al.* 2021). Fig. 12 depicts a comparison of measured and projected FMEP rates as a function of engine speed. The trend and magnitude are both well-matched.

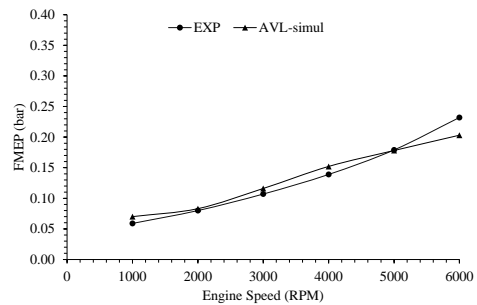


**Fig. 12. Comparison of FMEP predictions and measurements at various engine speeds.**

### 3.3. Effect of the Top Ring Tangential Force

As a simulated result, Fig. 13 depicts the lubrication oil consumption sources in the engine at various crank angles. As can be seen, there are two primary sources of oil consumption. The first one is the evaporation of oil inside the combustion chamber. The evaporation happens because the gas temperature, velocity, and heat transfer coefficient inside the combustion chamber are the highest during the engine operation, especially in the power stroke. All these factors lead to increase oil evaporation of the engine.

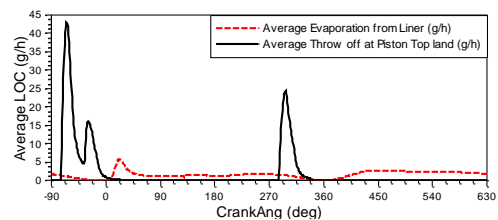


**Fig. 13. LOC sources.**

The other source is the amount of oil sprayed into the combustion chamber from the top surface of the first ring, which is located between the liner wall and the top land of the piston. As shown in Fig. 14, oil accumulates in the piston top land for several reasons as follows:

- Oil flows through the grooves on the upper and lower surfaces of the rings.
- Oil flows through the ring's end gap.

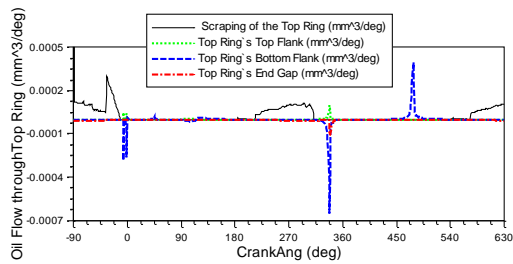
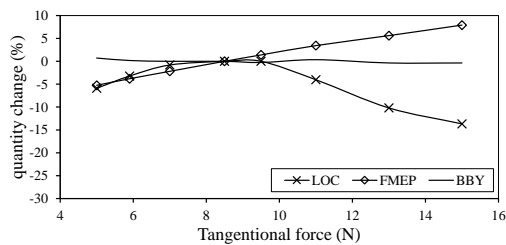


**Fig. 14. Top ring oil flow.**

- Oil scrapes against the first ring's face during the upward piston movement during the compression and exhaust strokes.

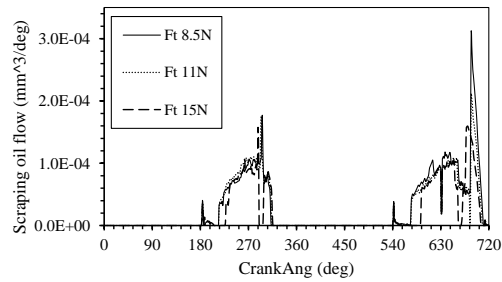
It can be concluded that most of the oil leaked into the combustion chamber was for the layer scraped due to the upwards piston movement in the compression (between CA -90 and 0 deg.) and exhaust stroke (between CA 270 and 360 deg.). The oil passes through the top ring groove and accumulates on the first piston land during the ring fluttering (near CA 280 deg.) and the pressure gradient between the upper and lower sides of the top ring.

Fig. 15 shows the impact of changing the top ring tangential forces on the lubrication oil consumption, Blow-by, and friction mean effective pressure. The simulation results show that increasing the top ring tangential force improves the first ring's sealing efficiency, thus reducing lubrication oil consumption. However, increasing the asperity contact pressure between the ring face and the liner wall increases friction power loss. Changing the radial force value reduces oil consumption by 14% while increasing friction by 8%. Changing the tangential force has no effect on the blow-by gases, as shown in Fig. 15. Because most gases flow through the end gap and top and bottom flanks of the top ring, and only a few, "almost none," flow through the ring face.



**Fig. 15. Effect of top ring tangential force on LOC, BBY, and FMEP.**

Fig. 16 depicts lubricant flow during compression ring scraping. Consider that increasing the tangential force from 8.5 to 15 Newton reduces oil flow by 15%. During compression, the tangential force acting on the top ring increases due to the increasing radial pressure applied to the back of the ring, where the piston moves upward at an angle of CA 540-720 degrees. The increase in radial forces cancels out the hydrodynamic force generated by the oil layer between the ring face and the cylinder liner.



**Fig. 16. Top ring scraping oil flow.**

### 3.4. Effect of the scraper ring tangential force and face geometry

Preventing combustion gases from leaking into the crankcase is the most important role of the ring pack system, performed mainly by the second piston ring as stated in the sensitivity analysis of this paper and consistent with findings in (Cavallaro *et al.* 2012; Delprete *et al.* 2019). As a part of studying the gas flow behavior at the second ring, Fig. 17 shows the blow-by gas escaping into the crankcase passing through the second scraper ring. The results of the gas flow model illustrated in Fig. 17 indicated that just 24% of the gas volume passes through the ring face during the piston movement while 76% through the ring end gap and the side surface. Also, the theoretical results indicate that approximately half of the blow-by gas passes through the second piston groove during the ring fluttering resulting from the piston movement and the distribution of the pressure applied to the surfaces of the ring.

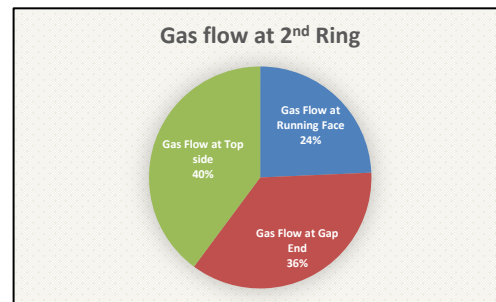


**Fig. 17. 2<sup>nd</sup> ring gas flow percentage.**

The effect of the second ring tangential force on blow-by gas flow, oil consumption, and FMEP is depicted in Fig. 18. The figure demonstrates that increasing the tangential force results in an 8% reduction in blow-by while increasing the friction between the ring face and the liner wall by 7%. However, the amount of oil consumed is still the same. Thus, it can be concluded that only 2% of the total Blowby gas is reduced by increasing the tangential forces of the ring from 8 to 13N, and it is considered a small percentage compared to the amount of increase in energy lost by friction. Otherwise, reducing the tangential force to 5N leads to a decrease in the FMEP to 5% while keeping oil consumption and Blow-by constant. The functional part of the second ring's role is to distribute the lubricant layer uniformly on the cylinder liner due to the special design of the ring face. The taper face shape of the ring increases the scraping efficiency

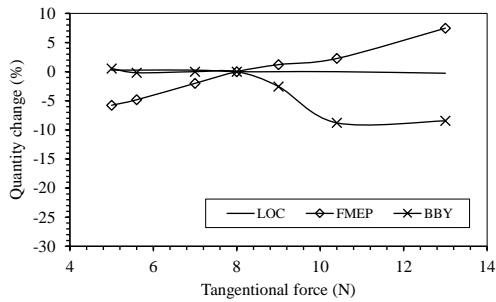


**Fig. 18. Effect of second ring tangential force on LOC, BBY, and FMEP parameters.**

and concurrently increases the sealing efficiency to prevent gas leakage. The effect of the tangential force of the second ring is considered to be slightly due to the difference in pressure applied at the top and bottom of the ring, as in most cases, the pressure in the upper part is greater or equal to the lower part. Thus, a small amount of the lubricating oil passes upward to the top ring.

Based on the literature and the simulation results, the ring face geometry can be adjusted to improve the system performance (Iijima *et al.* 2002; Delprete *et al.* 2019). The tapered face of the second scraper ring has been analyzed to calculate the sensitivity of the taper angle value on the amount of LOC, BBY, and FMEP parameters, as illustrated in Fig. 19. By varying the taper angle from 30' to 180', the LOC, BBY, and FMEP values can be calculated using a base design with a straight face (0 deg. taper angle). As can be seen in Fig. 19, the blow-by gas flow rate drops by 60% when the taper angle is increased from 0' to 60'. At the same time, the oil consumption and friction are reduced by about 20% and 10%, respectively. The results in Fig. 19 also show that increasing the tapered angle by more than 1 degree (60') has a limited effect on blow-by and friction. On the other hand, increasing the angle will reduce the scraping efficiency, thus increasing the oil consumption. The radial forces resulting from the gas pressure will reduce the effect of tangential forces in the opposite direction, which increases the oil accumulated between the first and second ring.

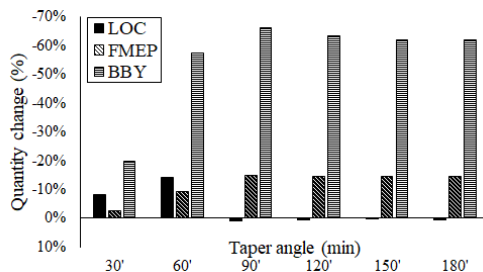


**Fig. 19. 2nd ring's taper face angle impact on LOC, BBY, and FMEP compared to base design.**

It can be concluded from the results above that changing the angle supports reducing the amount of gas flow through the ring face as well as reducing the LOC. The design of the ring face with a taper angle

could change the pressure distribution on the ring face, which divided the applied force results into radial and axial (radial hydrodynamic pressure and axial gas pressure), thus increasing the sealing capacity of the ring face. At the same time, the angle assists reduce the contact surface area between the ring face and the cylinder liner to reduce the amount of friction resulting from the asperity contact (as shown in Fig. 20). In other words, the radial force between the ring face and liner will reduce as the contact area is reduced, which helps reduce friction. At the same time, the presence of the tapered angle leads to converting a part of the gas force applied on the top of the ring into radial forces. Thus, this force helps to reduce the effect of the ring's forces on the liner, reducing friction and blow-by.

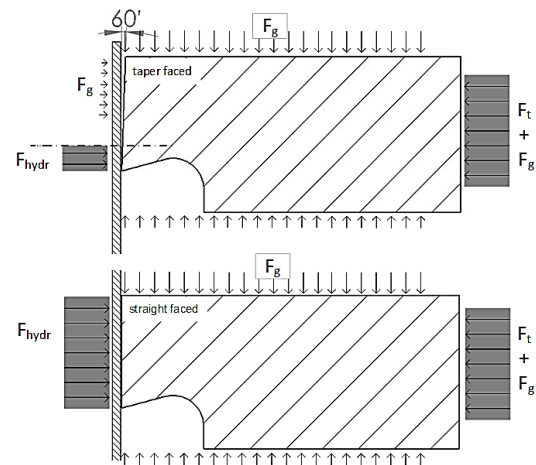


**Fig. 20. Distribution of the forces acting on the second ring surfaces with and without taper angle.**

### 3.5. Effect of the Oil Control Ring Tangential Force and Face Geometry

Several studies have examined the impact of tangential force on two- or three-piece oil control ring performance. Modifying the spring or expander design allows adding radial force to the piston ring without changing the basic dimensions of the oil ring geometry (Esser, 2002; Iijima *et al.*, 2002; GmbH, 2016b; Delprete *et al.*, 2019). The oil control ring creates a lubrication film between moving surfaces (the piston and rings face one side and the liner wall on the other) to reduce friction. Therefore, the tangential force value of the oil ring is large compared to the other rings. Fig. 21 depicts the influence of the oil control ring's tangential force on LOC, FMEP, and BBY. The results reveal that raising the force from 25 to 40 N decreases oil consumption by around 35% while increasing friction by approximately the same amount. Due to the high contact area between the ring and the liner, additional radial forces increase the friction rate between the contact surfaces, lower the lubrication gap created by hydrodynamic forces, and thus reduce the thickness of the oil layer dispersed on the cylinder wall. On the other hand, because the second ring is responsible for preventing combustion gases from escaping, the oil control ring has a negligible

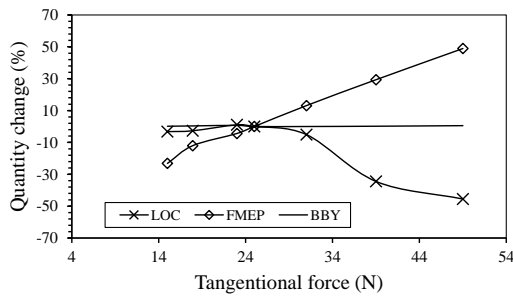


**Fig. 21. 3<sup>rd</sup> ring's tangential force impact on LOC, BBY, and FMEP.**

effect on blow-by gas flow. Thus, radial force has no effect in gas sealing.

It can be concluded from the sensitivity analysis that increasing the tangential force for all rings has an opposite role through reducing lubrication oil consumption and gas leakage (Blowby), thus increasing engine efficiency and reducing emissions. However, this is accompanied by increased friction (reducing the engine performance and increasing the emission by fuel consumption), especially in the face of the ring.

The oil control ring is considered the most effective in reducing oil consumption and increasing friction due to its design. Due to the large ring thickness, the contact area of the oil control ring with the liner wall is greater. As a result, three different oil control ring face profiles were chosen, and the tangential force effect was investigated. The design model was created without a face coating in order to investigate the effect of actual surface contact between the ring and the liner on the friction value.

Fig. 22 illustrates the FMEP and LOC change rate simulation findings for three different faces of the oil control ring profiles (DEF) in comparison to the default design. The results indicated that the LKZ design might significantly minimize oil consumption by 25% compared to other models. To reduce lubrication oil consumption, the oil control ring's scraping action must be improved, as the tapered profile of the ring's face helps minimize oil scraping during upward piston movement and also allows oil to accumulate in the gap between the ring face and the liner due to the tapered angle, which reduces oil consumption. Additionally, the contact edge's stepped surface improves downward scraping effort. This type then increases friction by 10%. As a result, coating the ring face makes it feasible to overcome the increase in friction (Dolatbadi *et al.*, 2020).

However, the results showed that the SSF ring design has an unfavorable effect on both friction and oil consumption compared to the default design, where the friction and oil consumption increased up to 10%. Fig. 23 shows the lubrication gap thickness and the average thickness generated due to the movement of the piston. The gap created between the oil control ring face and the liner surface reduces by changing the ring face's profile design, which improves the scraping effectiveness and thus reduces the amount of oil thrown to the upper rings.

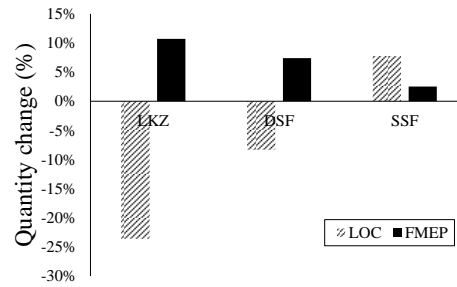


**Fig. 22. Face geometry effect rate compared with the reference design (DEF).**

Therefore, it can be seen that the sharp increases in the lubrication layer thickness shown in Fig. 23 after CA 0 degree in the downstroke due to the straight shape of the ring face in the SSF model profile without stepped surface. It should be noted that combining a stepped surface and taper of the LKZ ring provides better pressure distribution on the downstroke and a significantly small impact on the upstroke, which leads to control of the oil consumption (Powertrain, 2010).

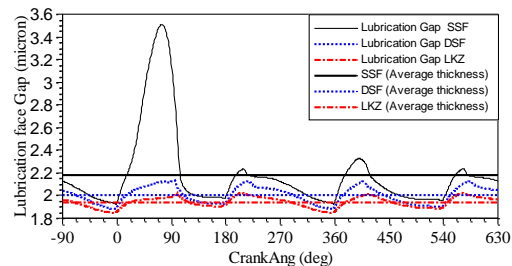
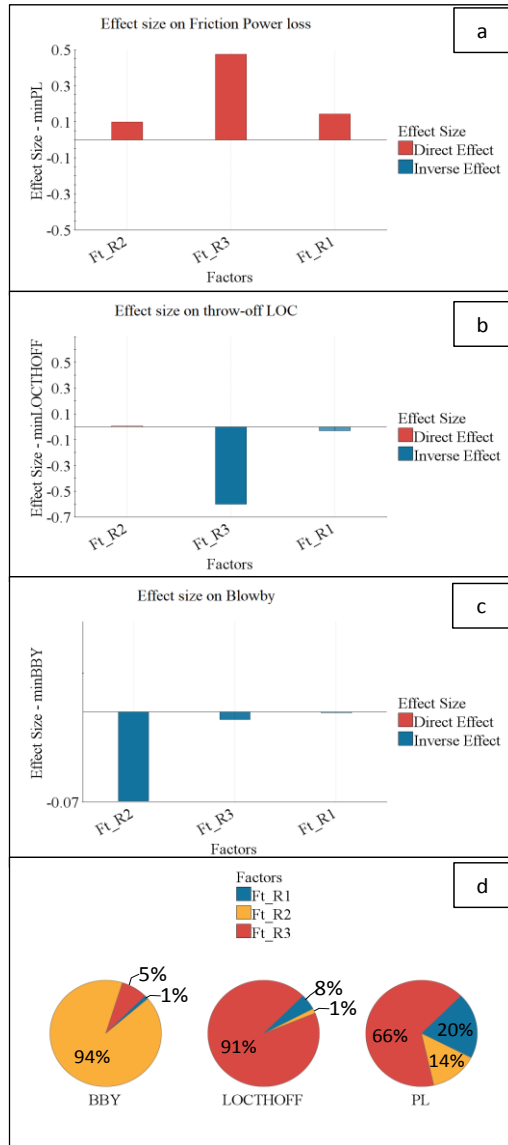


**Fig. 23. oil film thickness behavior of the different design.**

### 3.6. Sensitivity Analysis-modeFRONTIER

Extensive calculations were conducted to analyze the relative significance of several parameters affecting ring pack performance. Fig. 24. explained the strength of the relationship between the tangential forces as input variables and the LOCTHOFF, BBY, and FMEP as output variables. The positive effect size value directly relates to the output variables, and the negative value indicates an inverse relation. The modeFRONTIER tangential force sensitivity analysis indicates that the force between the piston rings directly affects the friction power loss. In opposite, it has an inverse effect on the amount of lubrication oil consumption and blow-by rate. In other words, increasing the tangential force increases friction and reduces the amount of oil consumption and blow-by.

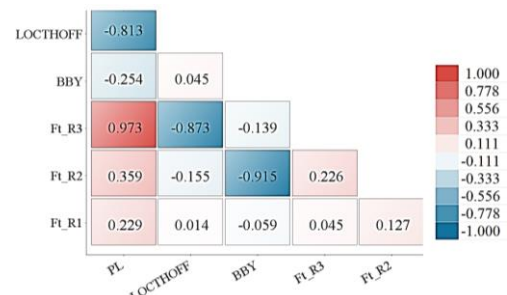
Additionally, the results indicated that gas sealing is not affected by the tangential force exerted by the first and third rings (as depicted in Fig. 24 b, c). This confirms that the blow-by gas mainly passes through the first piston groove (through the upper and lower flanks of the top ring), and the third ring's main function is to control the lubrication process. It is also interesting to note that increasing the radial force in the second ring significantly affects the gas sealing (as depicted in



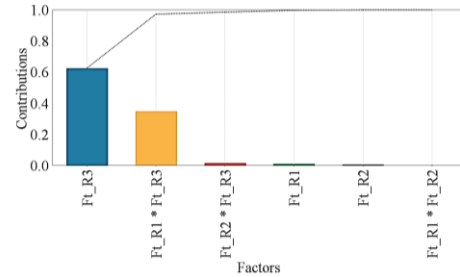
**Fig. 24. Effect of the input variables on (a) power loss (b) throw-off LOC (c) BBY (d) The sensitivity percentage of tangential forces on the output variables.**

Fig. 24 a), where about 24% of the gasses pass through the ring face. This value has been estimated by solving the ring dynamic model and finding the net radial force acting on the ring.

Furthermore, Fig. 25 shows the results of the correlation matrix of the different variables represented by the tangential forces, friction, blow-by gas, and the lubrication oil consumption rate. The matrix depicts the correlation between the factors, which is a powerful tool for summarizing a dataset, selecting the optimum design, and making decisions related to the piston-ring system. It can be concluded from the matrix that there is a high sensitivity inverse correlation between the change of friction power loss and oil consumption. This shows that changing the tangential force has the opposite effect on ring friction and oil consumption, as one objective increase while the other decreases. It is reversed and



**Fig. 25. Correlation matrix between the analyzed effective factors.**



**Fig. 26. Main and interaction effect of the tangential force on lubrication oil consumption.**

medium in intensity. Changing the oil consumption value with blow-by gas has a low sensitivity.

The statistical modeling algorithm SS-ANOVA has also improved interpretability and correlated main and interaction effects concepts for closer examination. The sensitivity analysis results in Fig. 26 show that the tangential force has a main and an interaction effect on lubrication oil consumption. The \* sign between the variables means that there is an interaction effect. This study's findings show that the oil control ring's tangential force is the most significant influence on oil consumption, followed by the interaction effect of radial forces related to both the top and third rings. This indicates that the changes in the tangential force of the top and oil rings are related, reflecting the importance of studying the sensitivity of factors using multi-objective optimization. It helps find a balance between changing the amount of tangential force to reach the optimum design.

#### 4. OPTIMIZATION RESULTS

The outcome of optimization Pareto diagram Fig. 27 depicts the design points distributed in two-dimensional space. At the same time, the bubble color represents the figure's third dimension, which represents the three non-dimensional objectives considered in the multi-objective optimization study, namely minimum oil consumption, power loss, and blow-by. The limit lines shown in the figure illustrate the value of respondent objectives computed by simulations and validated by experimental testing, which have a non-dimensional value of 1.

The design points distribution shows that the amount of blow-by gas is slightly affected by changing the

tangential forces, where the non-dimensional change ranges between 0.19-1.02. This change reflects the correctness of the sensitivity analysis in this study, which showed that only the second ring has a main effect on gas flow, and the ring face has the lowest amount, equivalent to 24% of the total gas. At the same time, the amount of lubrication oil consumption is more sensitive by a rate of  $\pm 0.1$  through the effect of tangential forces on the lubrication layer thickness and the scraping process. Although, the effect of the tangential force is the largest concerning friction through increasing the asperity contact between the ring face and the liner by a rate of  $\pm 0.3$ . The above values describe the major challenge of reducing oil consumption while not increasing friction, which is the study's primary objective.

The Pareto method was used in the multi-objective optimization study. The Pareto method uses dominance to identify dominant and non-dominated solutions and keeps the solution vectors independent during optimization. The dominance solution and optimal rate are commonly achieved when one objective function cannot be reduced without increasing the other objectives. The results show some force value selection options. Tangential force can be chosen based on oil consumption, power loss or blow-by, or a combination of the three. As shown in Fig. 27, the optimal value is determined by minimizing the distance from the original point.

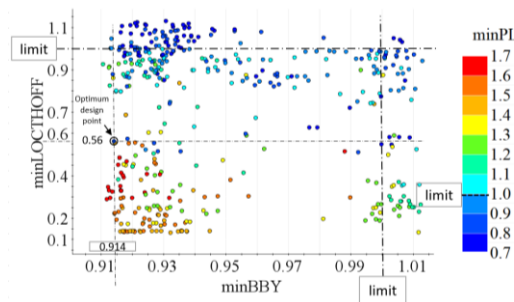


**Fig. 27. Two-dimensional design points distribution of the optimization study.**

As explained in the above results, changing the amount of tangential force of the top and second rings requires a change in the geometry of the ring or

the type of material. Therefore, when choosing the appropriate design resulting from the optimal point, adjustments must be made in proportion to the values of the resulting forces. The proposed design in this paper involves increasing the tangential forces of the top ring by 3 N and the second ring by 5 N, as shown in Table 7. The radial thickness of the upper ring was changed to 0.4 mm and the face width to 0.03 mm, as well as the radial thickness of the second ring to 0.6 mm and the face width to 0.05 mm, to obtain the required tangential force values based on Eq. 8. Changing the ring radial width by a larger amount than the face thickness has been suggested to avoid increasing the friction between the liner and the ring face. Despite this, there is an increase in the friction as well as the blow-by after making geometry modifications. As a result, to increase the surface area of the upper and lower ring flanks. Thus, the proposed design reduced oil consumption by up to 30% while increasing friction and blow-by by 0.8 and 2%, respectively, which can be considered the original objective of the optimization study presented in this research.

### 5. CONCLUSIONS

This article conducted a sensitivity study of the parameters impacting the sealing performance of piston and cylinder assembly. The genetic algorithm was used to conduct multi-objective optimization research in order to provide the optimal design for the piston and ring system. This study utilized the AVL Excite simulation model for a gasoline engine piston-ring assembly and the ModeFRONTIER optimizer. The following are the findings:

- Increasing the top ring tangential force improves the first ring sealing. It also reduces friction. An increase in force value reduces oil consumption by 14% but increases friction by 8%. Changing the top ring's tangential force had no effect on blow-by gas.
- Increasing the second ring tangential force reduces blow-by by 8% while increasing liner wall friction by 7%. However, oil consumption is unaffected. Additionally, the angle of the second compression ring has a significant effect on preventing upward scraping, which results in reduced oil consumption. Where the 60° angle is the optimal selection.

**Table 7 Optimal configuration performances relative to the baseline**

|                                            | Factors  |         |         | Responses     |               |                 |
|--------------------------------------------|----------|---------|---------|---------------|---------------|-----------------|
|                                            | Ft1 (N)  | Ft2 (N) | Ft3 (N) | LOC (g/h)     | BBY (l/min)   | FMEP (N)        |
| Engine default design                      | 6.5-10.5 | 6.5-9.5 | 21-29   | ~14           | ~22.2         | ~0.265          |
| Optimal design from modeFRONTIER results   | 11.7     | 13      | 15      | ~11           | ~21.7         | ~0.23           |
| Responses percentage change                | -        | -       | -       | 25% Reduction | 2% Reduction  | 13% Reduction   |
| Optimal design after geometry modification | 10-15    | 9.5-13  | 15-17   | ~10           | ~22.7         | ~0.267          |
| Responses percentage change                | -        | -       | -       | 30% Reduction | 2% Increasing | 0.8% Increasing |

- Increasing the oil control ring tangential force from 25 to 40 N reduces oil consumption by about 35% while increasing friction by about the same amount. However, the blow-by gas is unaffected. Also, The LKZ design could significantly reduce oil consumption by 25% compared to the other types, while increasing friction by about 10%.
- According to the sensitivity analysis, studying the interaction effect of the forces as an integrated system yields more accurate results in developing ring assembly performance. As a result, the interaction effect of radial forces related to the top ring and the oil control ring is more sensitive to oil consumption. This is an important finding not hitherto reported in the literature.
- The sensitivity analysis showed that the tangential forces directly affect friction power loss and an inverse effect on both oil consumption and blow-by.
- The multi-objective optimization study applied in this paper succeeded in proposing a modification to the value of tangential forces that helps reduce oil consumption by up to 30% with a slight increase in the amount of friction 0.8%.

#### ACKNOWLEDGMENT

The authors would like to appreciate Irankhodro Powertrain Company (IPCo) and Ring Khodro Pars Company (RKP) for their full financial and technical support of this research. The authors also appreciate the technical support from Mr. Reza Soltani the head of CAE department and Dr. Seyed Ashkan Mosavian of engine Labs Unit, Irankhodro Powertrain Company (IPCo) in many related areas.

#### REFERENCES

- Abu-Nada, E., I. Al-Hinti, A. Al-Sarkhi and B. Akash (2008). Effect of piston friction on the performance of SI engine: a new thermodynamic approach. *Journal of Engineering for Gas turbines and power* 130(2)
- Ahmed Ali, M. K., H. Xianjun, R. Fiifi Turkson and M. Ezzat (2016). An analytical study of tribological parameters between piston ring and cylinder liner in internal combustion engines. *Proceedings of the Institution of Mechanical Engineers, Part K: Journal of Multi-body Dynamics* 230(4), 329-349.
- Almansoori, A. Q., A. Hajjalimohammadi, S. M. Agha Mirsalim and S. Alizadehnia (2017). A novel experimental test rig for simulating of the fuel injection system components behavior under cold conditions. *The Journal of Engine Research* 47(47), 31-38. (Research Study)
- Bewsher, S., M. Mohammadpour, H. Rahnejat, G. Offner and O. Knaus (2019). An investigation into the oil transport and starvation of piston ring pack. *Proceedings of the Institution of Mechanical Engineers, Part J: Journal of Engineering Tribology* 233(1), 112-124.
- Cavallaro, G., F. Demesse and P. D. Masson (2012). Internal Combustion Engine Blow-by Modeling: Importance of Thermal Environment Simulation for an Accurate Prediction SAE 2012 International Powertrains, Fuels & Lubricants Meeting No. 2012-01-1751. *SAE International*.
- Clarich, A., M. Carriglio, G. Bertulin and G. Pessl (2016). Connecting rod optimization integrating modeFRONTIER with FEMFAT. In: 6-th BETA CAE International Conference. [https://www.beta-cae.com/events/c6pdf/12A\\_3\\_ESTECO.pdf](https://www.beta-cae.com/events/c6pdf/12A_3_ESTECO.pdf)
- Delprete, C., E. Selmani and A. Bisha (2019). Gas escape to crankcase: impact of system parameters on sealing behavior of a piston cylinder ring pack. *International Journal of Energy and Environmental Engineering* 10(2), 207-220.
- Di Battista, D. and R. Cipollone (2016). Experimental and numerical assessment of methods to reduce warm up time of engine lubricant oil. *Applied Energy* 162, 570-580.
- Dolatabadi, N., M. Forder, N. Morris, R. Rahmani, H. Rahnejat and S. Howell-Smith (2020). Influence of advanced cylinder coatings on vehicular fuel economy and emissions in piston compression ring conjunction. *Applied Energy* 259, 114129.
- Elsharkawy, A. A. and S. F. Alyaqout (2009). Optimum shape design for surface of a porous slider bearing lubricated with couple stress fluid. *Lubrication Science* 21(1), 1-12.
- Esser, J. (2002). Oil control rings and their effect on oil consumption. *MTZ worldwide* 63(7-8), 22-25.
- Froelund, K. and E. Yilmaz (2004). Impact of engine oil consumption on particulate emissions. In: *ICAT international conference on automotive technology*, Istanbul, Turkey
- Gholami, R., H. Ghaemi Kashani, M. Silani and S. Akbarzadeh (2020). Experimental and Numerical Investigation of Friction Coefficient and Wear Volume in the Mixed-Film Lubrication Regime with ZnO Nano-Particle. *Journal of Applied Fluid Mechanics* 13(3), 993-1001.
- GmbH, A. L. (2016a). *EXCITE Piston&Rings – Theory*, AVL.
- GmbH, M. (2016b). *Engine testing, Pistons and engine testing*. Springer Fachmedien Wiesbaden, Wiesbaden. pp. 115-280.
- Gunantara, N. (2018). A review of multi-objective optimization: Methods and its applications. *Cogent Engineering* 5(1), 1502242.
- Iijima, N., T. Miyamoto, M. Takiguchi, R. Kai and M. Sato (2002). An experimental study on

- phenomena of piston ring collapse. *SAE Transactions*, 1019-1026.
- Jahromi, H. (2014). *Sensitivity analysis of CFD method with modeFRONTIER*. MS thesis, Department of Applied Mechanics, Chalmers University of Technology, Göteborg, Sweden.
- Jena, S. (2013). *Multi-objective optimization of the design parameters of shell and tube type heat exchanger based on economic and size consideration*. B.Tech. Thesis, National Institute of Technology, Rourkela.
- Kaliappan, A., S. Mohanamurugan and P. Nagarajan (2019). Numerical investigation of sinusoidal and trapezoidal piston profiles for an IC engine. *Journal of Applied Fluid Mechanics* 13(1), 287-298.
- Kirner, C., J. Halbhuber, B. Uhlig, A. Oliva, S. Graf and G. Wachtmeister (2016). Experimental and simulative research advances in the piston assembly of an internal combustion engine. *Tribology International* 99, 159-168.
- Lu, Y., C. Liu, Y. Zhang, J. Wang, K. Yao, Y. Du, and N. Müller (2018). Evaluation on the tribological performance of ring/liner system under cylinder deactivation with consideration of cylinder liner deformation and oil supply. *PLoS one* 13(9):e0204179.
- Menacer, B. and M. Bouchetara (2020). The compression ring profile influence on hydrodynamic performance of the lubricant in diesel engine. *Advances in Mechanical Engineering* 12(6):1687814020930845. doi: 10.1177/1687814020930845
- Miao, R., G. Jing, X. Zeng and H. Ge (2020). Optimization of Piston-Ring System for Reducing Lube Oil Consumption by CAE Approach. 0148-7191, SAE Technical Paper.
- Mishra, P. C. and S. Kumar (2019). Modeling for design optimization of piston crown geometry through structural strength and lubrication performance correlation analysis. *Frontiers in Mechanical Engineering* 5:17.
- Mohiuddin, A., M. Rahman and Y. H. Shin (2011). Application of multi-objective genetic algorithm (MOGA) for design optimization of valve timing at various engine speeds. In: *Advanced Materials Research* 1719-1724.
- Patir, N. and H. Cheng (1979). Application of average flow model to lubrication between rough sliding surfaces. *ASME Journal of Lubrication Technology* April 1979 101(2), 220-229.
- Powertrain, F. M. (2010). Piston ring improves fuel economy and reduces emissions. *Sealing Technology* 2010(10), 2-3.
- Qian, Y., Q. Hu, Z. Li, S. Meng, K. Zhu, X. Cheng and C. Tao (2020). An experimental investigation on the evaporation characteristics of lubricating oil film in different grooves. *International Communications in Heat and Mass Transfer* 110, 104413.
- Rahmani, R., H. Rahnejat, B. Fitzsimons, and D. Dowson (2017). The effect of cylinder liner operating temperature on frictional loss and engine emissions in piston ring conjunction. *Applied Energy* 191, 568-581.
- Saligheh, A., A. Hajjalimohammadi and V. Abedini (2020) Cutting forces and tool wear investigation for face milling of bimetallic composite parts made of aluminum and cast iron alloys. *International Journal of Engineering* 33(6), 1142-1148.
- Smith, E. H. (2011). Optimising the design of a piston-ring pack using DoE methods. *Tribology international* 44(1), 29-41.
- Soejima, M., Y. Harigaya, T. Hamatake and Y. Wakuri (2017). Study on Lubricating Oil Consumption from Evaporation of Oil-Film on Cylinder Wall for Diesel Engine. *SAE International Journal of Fuels and Lubricants* 10(2), 487-501.
- Sohrabiasl, I., M. Gorji-Bandpy, A. Hajjalimohammadi and M. A. Mirsalim (2017). Effect of open cell metal porous media on evolution of high pressure diesel fuel spray. *Fuel* 206, 133-144.
- Tian, T., V. W. Wong and J. B. Heywood (1996). A piston ring-pack film thickness and friction model for multigrade oils and rough surfaces. *SAE transactions*, 1783-1795.
- Turnbull, R., N. Dolatabadi, R. Rahmani and H. Rahnejat (2020). An assessment of gas power leakage and frictional losses from the top compression ring of internal combustion engines. *Tribology International* 142, 105991.
- Usman, A., T. Ahmad Cheema and C. Woo Park (2015). Tribological performance evaluation and sensitivity analysis of piston ring lubricating film with deformed cylinder liner. *Proceedings of the Institution of Mechanical Engineers, Part J: Journal of Engineering Tribology* 229(12), 1455-1468.
- Vaghar, M. M., A. Moosavian and M. A. Ehteram (2021). An experimental and theoretical investigation on the effects of piston clearance and oil viscosity on Cranktrain friction. *Proceedings of the Institution of Mechanical Engineers, Part E: Journal of Process Mechanical Engineering* 235(6), 2230-2239.
- Venkataraman, P. (2009). *Applied optimization with MATLAB programming*. John Wiley & Sons.
- Zhang, Z., J. Liu, Y. Tang and X. Meng (2016). Optimizing the shape of top piston ring face using inverse method. *Industrial Lubrication and Tribology*.